ECCOMAS Congress 2016
VII European Congress on Computational Methods in Applied Sciences and Engineering
M. Papadrakakis, V. Papadopoulos, G. Stefanou, V. Plevris (eds.)
Crete Island, Greece, 5–10 June 2016

SEISMIC RETROFIT OF EXISTING BUILDINGS THROUGH THE DISSIPATIVE COLUMNS

Paolo Castaldo [(1)], Bruno Palazzo [(1)], Francesco Perri [(1)], Ivana Marino [(1)], Marco Maria Faraco [(2)]

[1] Department of Civil Engineering, University of Salerno.
via Giovanni Paolo II 132, 84084 Fisciano (SA), Italy
e-mail: {pcastaldo,palazzo,fperri,imarino}@unisa.it

[2] Department of Civil Engineering, University of Salerno.
via Giovanni Paolo II 132, 84084 Fisciano (SA), Italy
e-mail: mfaraco@hotmail.it

Keywords: Hysteretic Damper, Seismic Damage Reduction, Passive Energy Dissipation

Abstract. *A new replaceable hysteretic damper to better control seismic building damage, consisting of two or more adjacent steel vertical elements (columns) connected to each other with continuous mild/low strength steel shear links, is investigated in this study. New Dampers, called Dissipative Columns (DC), are continuously linked with X-shaped steel plates and provide additional stiffness and damping to a lateral system. The Dissipative Column has been conceived as a device installed within a frame or as an external damper to provide macro-dissipation. In fact, considering different configurations, a parametric analysis is developed, through non-linear pushover and cyclic analyses carried out in ABAQUS, in order both to evaluate the effect of the main geometrical and structural parameters and provide the design capacity curves of this new damper. Moreover, non linear dynamic analyses of an existing building without and with the Dissipative Columns have been performed in SAP2000 in order to evaluate the supplemental damping provided by the new damper. The DC can be considered a new damping device, easy to install in new as well as existing buildings in order to protect them from seismic damage.*

1 INTRODUCTION

Strong earthquakes have shown that a large percentage of buildings in the affected areas, even if properly built and designed according to the most advanced codes, suffer such severe damages [1] that they need to be demolished after the quake, since they would be expensive to repair. As is known, the acceptance of such level of damage due to severe earthquakes is related to the ductility-based design criteria that assume design seismic actions decrease by reduction factors. This approach may lead to high social and economic costs to the affected communities, and to a long recovery time for essential services and production activities. Inspired by new performance criteria, there is a growing belief that code design criteria are not sustainable for the high level of accepted damage, are impossible to repair, and that common buildings should be designed with a higher performance level. At the beginning of this century, Performance Based Engineering [2] introduced new principles with the scope to select more articulated targets better corresponding to different building roles and use, defining a variety and complex subdivision of performance objectives for seismic events with different intensities and frequencies of occurrence. The "Direct Displacement Based Design" philosophy [3] relates the specified performance level to the strain or drift limits for a specified seismic intensity. With the scope of minimizing structural damage, several frictional isolation devices [4]-[6] and dampers [7]-[8], new replaceable hybrid composite or steel devices [9]-[14] have been recently proposed as well as integrated design approaches [15]-[16] and new strategies, i.e., based on the collapse mechanism control [17]-[30] or energy balance [31], have been developed in order to dissipate seismic input energy outside of the primary structure. Dampers should absorb a significant portion of the input energy reducing the hysteretic energy demand to the primary structural elements. Another damper employed to dissipate energy dynamic energy through stable hysteretic behavior [32] consists in the buckling-restrained braces (BRBs). In [33], Low Yielding Strength (LYS) steel is investigated for improving the ductility capacity of box-shaped steel bridge piers and experimental work is carried out for four specimens having different thickness and sectional configurations for cyclic loading test. The test results reveal that the LYS steel portion with longitudinal stiffeners greatly improves the strength and ductility capacity of box columns and it is observed that LYS steel has a great cyclic strain-hardening characteristic. The advantage of use of LYS steel is that it can effectively use large plastic deformation in component plates and the failure of column is concentrated at the LYS steel segment and the energy dissipation occurs far beyond the yield point.

The aim of this paper is to investigate a new replaceable hysteretic damper having a basic form of the art of building, minimally architecturally invasive, consisting of two or more dissipative steel columns directly connected to two floors linked to each other with X-shaped low/mild steel plates. It will be shown that the new element is able to add significant stiffness and damping to the structural system to reduce seismic response and damage in primary structural members under severe earthquakes. A similar concept is used when Reduced Beam Sections (RBS) are realized at beam ends of a steel moment resisting frames. In fact, in this case the beam section resistance reduction is obtained by trimming the flanges, realizing the so called "dog-bone" [34]-[35]. The Dissipative Columns (DC) element will be investigated through non-linear pushover and cyclic analyses in ABAQUS [36]-[37] in order to characterize the local and global behaviour of the device considering different steel grades. These analyses are useful to design the yielding properties of the proposed damper depending both on the characteristics of the primary structure and the expected performance as discussed by [38]. The efficiency of the proposed damper applied on the benchmark system is investigated through time history analyses in SAP2000 [39].

2 MECHANICAL PRINCIPLES OF THE DISSIPATIVE COLUMN

The Dissipative Column model, as shown in Figure 1, can be considered as a sort of framed bi-pendulum with height equal to H, connected in parallel to the primary structure, able to react to the story drift Δ with a lateral force Q_D adding stiffness, strength and damping [12]-[13]. The design concept of the DC element aims to obtain a lever mechanism by which a small inter-story drift provides an amplified vertical drift between the X-plate ends (Figure 1) reacting with shear forces. The X-shaped steel plates made of mild or Low Yielding Strength steel, having length a, thickness t, width at the ends b and vertical distance i, are also used as shear links between coupled elements.

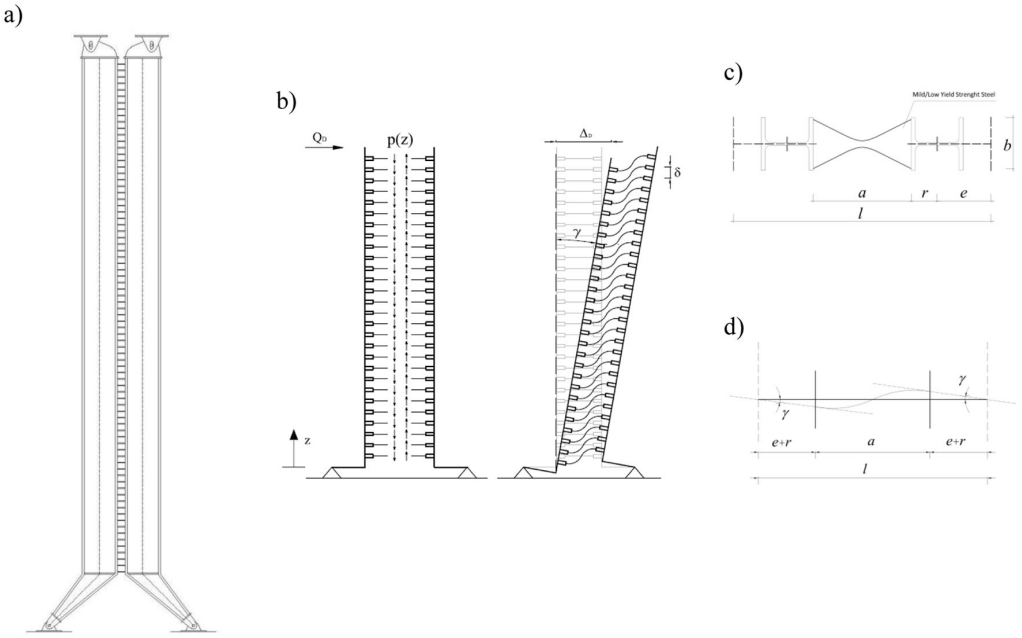

Figure 1: Eccentric Dissipative Column (a), structural model (b) and dissipative amplified mechanism (c)-(d).

Each lever arm is characterized by an eccentricity e, while, r is the rigid element representing half section of each column (Figure 1). The top ends of the model are linked to the upper floor through slotted bolted connections to allow large vertical displacements. By yielding a large volume of steel, the shear devices are able to dissipate substantial input energy during earthquakes, while also increasing damping in the entire system with the aim to reduce the damage in the primary system. With reference to reinforced concrete structures, the limit values of Inter-Story Drift Angle (ISDA) corresponding to different structural performance levels are suggested by Ghobarah [40]. The great advantages of the DC, if compared with classical steel dissipative braces [32], are the reduced architectural invasiveness, so that it is able to be integrated in any building, the ease of installation everywhere, replacement after earthquakes and the stable behavior in cyclic reversal deformation. To the scope to this study, two steel are considered to model the ADAS mechanical properties. In particular, S235 and LYP100 (Low Yield Point) are implemented, while the DC are totally conceived in S355.

3 SIMPLIFIED MECHANICAL BEHAVIOUR OF THE DC

As extensively discussed in [13], the vertical drift δ between the ends of a generic shear link in the elastic range, being the curvature χ constant along each half plate, is related to shear force V_d developed by each X-shaped plate, as:

$$\delta = 2\int_0^{a/2}\int_0^{a/2} \chi(x)dxdx = \frac{3}{2}\frac{a^3}{Ebt^3}V_d \tag{1}$$

where a, t, b are, respectively, the X-plate length, thickness, width at the ends and E is Young's modulus of the steel plates. The axis x represents the barycentric axis of a generic steel plate. Hence, the single X-plate vertical stiffness is equal to:

$$K_d = \frac{V_d}{\delta} = \frac{2}{3}\frac{Ebt^3}{a^3} \tag{2}$$

In the case of small eccentricity, a simplified analysis of the DC behavior subjected to relative displacements can be easily carried out assuming that the column flexural deformation is negligible respect to the case of flexible inextensible links. An inter-story drift produces a shear drift angle γ and vertical drifts δ along the X-shaped steel plate. Under such simplified assumptions, for the equilibrium, the top-base relative displacement Δ of a DC element with height H is related to the drift angle γ as:

$$\Delta = \gamma \cdot H \tag{3}$$

Therefore, each X-plate undergoes a vertical drift equal to:

$$\delta = (l-a)\,\Delta/H \tag{4}$$

where l represents pin axes distance (Figure 1). Therefore, the uniform distributed vertical load, along the vertical axis having origin in the hinge (Figure 1), due to the shear drift angle γ applies:

$$p = \frac{2}{3}\frac{Ebt^3}{a^3 i}(l-a)\,\Delta/H \tag{5}$$

where i represents the plates vertical distance. The term $(l-a)/2 = r$ represents a small lever arm that can be amplified using eccentricity e between the vertical axis and the supports as will be shown in the following. The axial force at the base of each column is equal to:

$$N_c = \frac{2}{3}\frac{Ebt^3}{a^3 i}(l-a)H\,\Delta/H \tag{6}$$

According to the experimental tests [41]-[42], the load-deformation curve of the X-shaped mild steel plates can be idealized as a bilinear curve with a ratio of post yielding stiffness to the initial one equal to 0.03 and available displacement ductility ratio $\mu=\delta/\delta_y$ varying in the range between 3 and 5 [43]. Since yielding strength f_y is reached almost uniformly along the device, the yielding vertical load p_y can also be expressed as:

$$p_y = \frac{2M_{d,y}}{ia} = f_y\frac{bt^2}{2ia} \tag{9}$$

while, the relative yielding displacement of each link can be written as:

$$\delta_y = \frac{V_{d,y}}{K_d} = f_y\frac{3a^2}{4Et} \tag{10}$$

Therefore, the lateral yield strength of the doubly hinged DC element can be evaluated as:

$$Q_{Dy} = f_y \frac{blt^2}{2ia} \tag{11}$$

and the yielding displacement applies:

$$\Delta_y = \frac{3}{4}\frac{f_y}{E}\frac{a^2 H}{t(l-a)} \tag{12}$$

Moreover, in presence of a significant eccentricity the column flexural deformation should not be neglected, therefore, as extensively described in [13], the top-base relative displacement Δ and lateral force of the DC element can respectively be expressed as:

$$\Delta = \gamma \cdot H + Q_D\left(\frac{eH^3}{3EI_c l} + \frac{e^2 H^2}{2EI_e l}\right) \tag{13}$$

$$Q_D = \frac{N_c l}{H} = \frac{\frac{2}{3}\frac{Ebt^3}{a^3 i}\gamma(l-a)H\frac{l}{H}}{1-\left[\frac{2}{3}\frac{Ebt^3}{a^3 i}\frac{l}{H}\left(2\frac{H^2}{l}\frac{e^3}{3EI_e}+\frac{H^2}{l}\frac{e^2}{EI_e}r+\frac{e}{l}\frac{H^3}{3EI_c}r\right)\right]} \tag{14}$$

where K_D represents the lateral stiffness of the Dissipative Column is given by:

$$K_D = \frac{2}{3}\frac{Ebt^3}{a^3 i}\frac{l}{H}(l-a) \tag{15}$$

Therefore, the stiffness ratio between the lateral stiffness of the Dissipative Column and the single X-plate vertical stiffness is equal to:

$$\frac{K_D}{K_d} = 2\frac{(a+2(e+r))}{H}(e+r) \tag{16}$$

4 NON LINEAR ANALYSIS OF THE X-SHAPE STEEL PLATES

Non-linear analyses in ABAQUS [36]-[37] are performed in order to characterize the non-linear behavior of the X-shape steel plates. In Table 1, the geometric and mechanical properties are reported with reference to two different steel grades: S235 [44] and LYP100 [33],[45].

Plate Length a [mm]	Plate Thickness t [mm]	Plate Width b [mm]	Plate Yield Stress f_y [N/mm^2]
150	15	120	132
150	15	120	235

Table 1: Geometrical and structural properties of the X-shaped steel plates.

Figure 2 shows the geometric shape as well as the deformed shape of the steel plates. A FE model has been defined in ABAQUS [36]-[37] with means of 3D elements with nonlinear stress-strain behaviour. The geometric model proposed by [46] has been adopted for the X-shape steel plates.

The displacement-controlled pushover analyses of the X plates have been performed until to reach 50 mm in terms of relative displacement and the corresponding curves related to the two different steel grades are plotted in Figure 3.

The results clearly show that in the case of LYP100 steel grade the yielding point has been firstly reached against to the case of S235 steel grade, but it is also evident that, in this case, the stiffness is larger with the effect that larger is, in the global model, as detailing described in the following, the additional shear forces on the steel vertical elements of the DC.

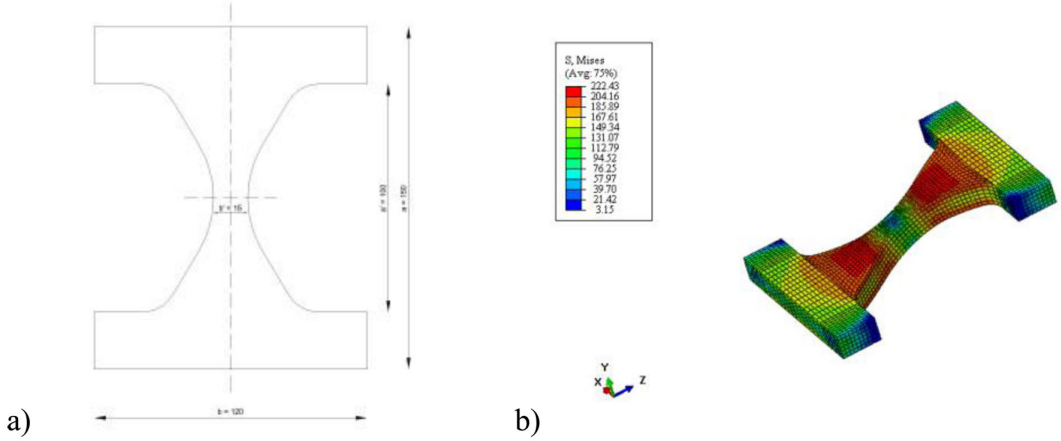

Figure 2: Geometric shape (a) and deformed shape (b) of a X-shaped steel plate.

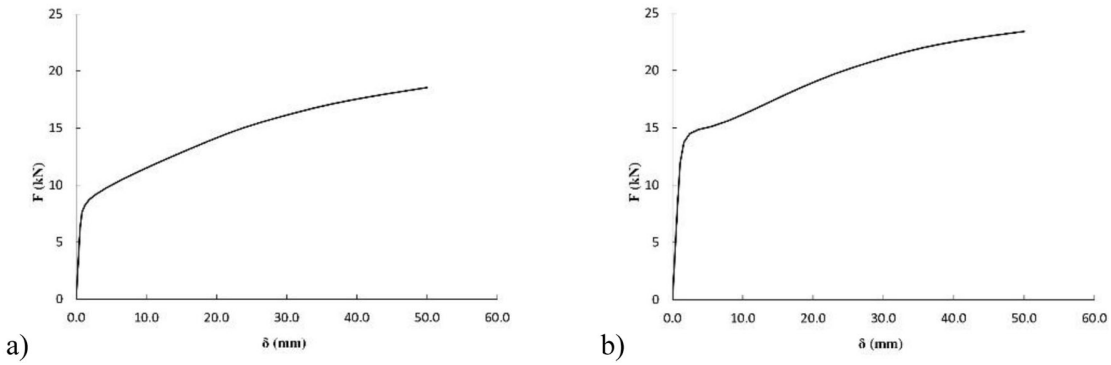

Figure 3: Pushover curves of the X plates: (a) LYP100 steel grade [33],[45]; (b) S235 steel grade [44].

5 NON LINEAR ANALYSIS OF THE DISSIPATIVE COLUMN

Defined the non-linear behavior of the X-shape steel plates, non-linear static and dynamic analyses of the Dissipative Column have been performed in ABAQUS [36]-[37]. In Table 2, the main geometric and mechanical properties of the DC are reported.

Height H	Column Distance *l*	Plate Length *a*	Plate Thickness *t*	Plate Distance *i*	Plate Width *b*	LYP 100 X-shape Yield Stress f_y	S235 X-shape Yield Stress f_y	Eccentricity *e*	Column Profile
[mm]	[mm]	[mm]	[mm]	[mm]	[mm]	[N/mm^2]	[N/mm^2]	[mm]	
10500	1650	150	15	125	120	132	235	400	ISE700

Table 2: Geometrical and structural properties of the Dissipative Column (DC).

A FE model has been defined in ABAQUS with means of 3D elements with nonlinear stress-strain behaviour [36]-[37]. As shown in Figure 4, in ABAQUS [36]-[37] it has been possible to carefully model the restrains at the base and the top of DC as well as the contact between the pin and the slotted holes. In particular, the hinge at the top of the DC (Figure 4a) has been modeled implementing an appropriate slotted hole in the superior plate in order to

simulate the sliding due to the applied displacement to the pin causing translation of the base system. In Figure 4(b) it is also shown the connection at the base of the DC. The FE points belonging to the internal surface of the inferior hinges have rigidly been connected to the reference point located in the center of the pin with the aim to simulate the free rotation in the plane.

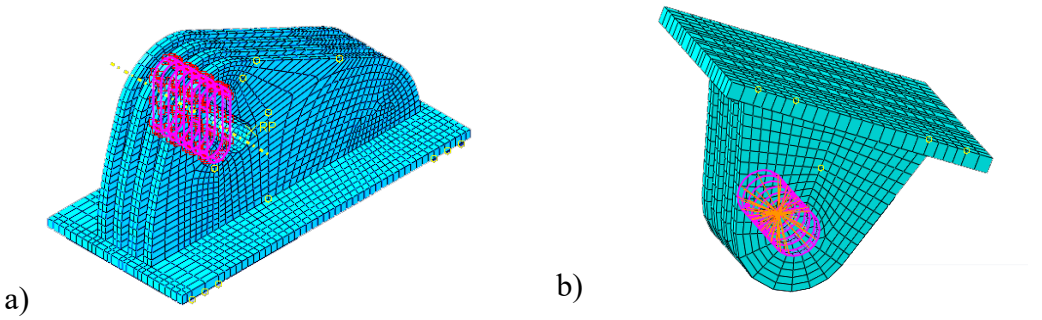

Figure 4: (a) Connection pin-hinge at the top of the DC; (b) Fix hinge at the base of the DC modeled in ABAQUS [36]-[37].

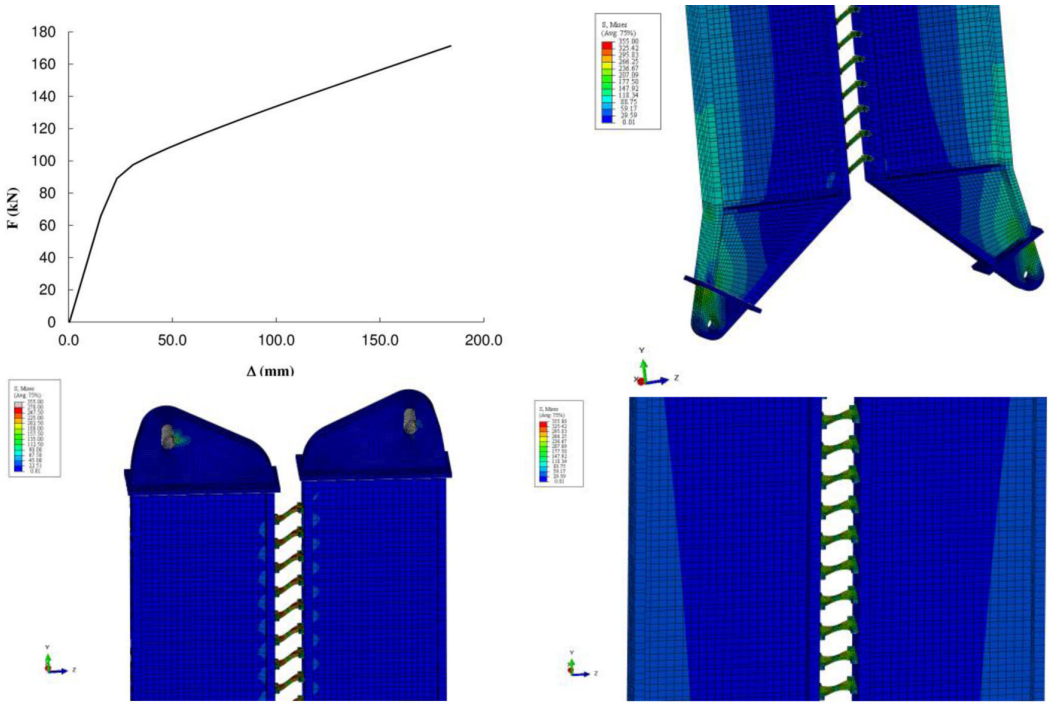

Figure 5: Pushover curve of the DC, using LYP100 X-plate, and deformed shape in ABAQUS [36]-[37].

Within nonlinear static analyses, in order to simulate the mechanical properties of the steel elements, a quadrilinear constitutive law [47] for S235 steel (X-shape plates) and S355 steel (vertical elements DC), while, a trilinear constitutive law regarding the LYP100 steel (X-shape plates) have been implemented in ABAQUS [36]-[37]. Figure 5 illustrates the geometric shape as well as the deformed shape of the DC. The displacement-controlled pushover analyses of the DC using LYP100 X-shape has been carried out until to reach 180 mm in terms of relative displacement as plotted in Figure 5, showing a yielding point at about 20 mm (0.17%). Figure 6 shows the comparison between the push-over curves of DC using LYP100 and S235 X-shape plates. The results demonstrate that in the case of LYP100 X-shape plates

the yielding point has been firstly reached against to the case of S235 X-shape plates, and the shear forces are lower although the lateral global stiffness remains the same.

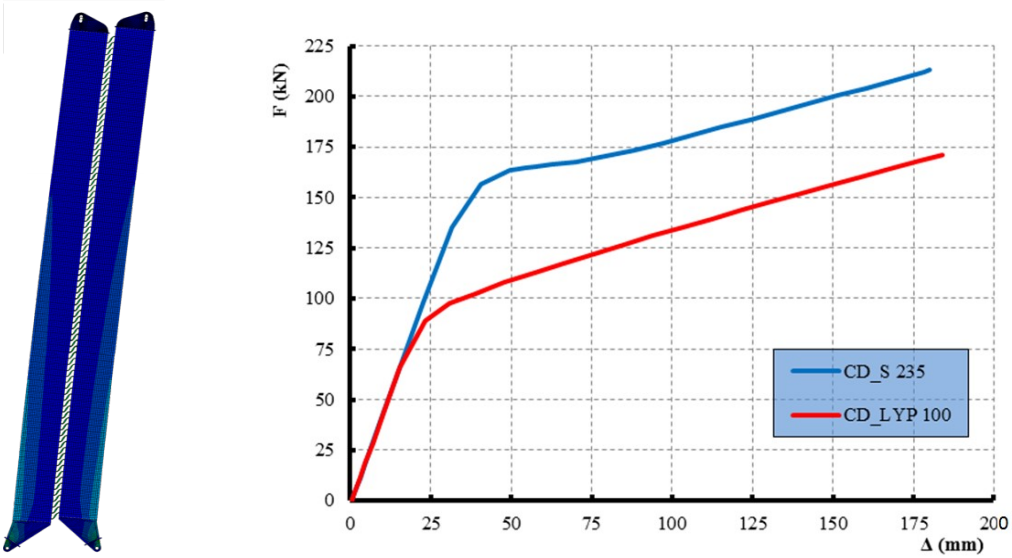

Figure 6: Pushover curve of the DC, using LYP100 and S235 X-shape plates, and deformed shape in ABAQUS [36]-[37].

In order to also simulate the behavior under seismic loads, the nonlinear behaviour of the X-shape plates has been described by a nonlinear kinematic hardening model in the case of nonlinear cyclic analyses. In particular, the nonlinear cyclic analyses has been performed until to reach a value of ductility equal to 10 in plastic range. As previously discussed, all the analyses of the DC are performed considering LYP100 and S235 X-shape plates. Figure 7 shows the results of displacement-controlled nonlinear cyclic analyses of the DC equipped with LYP100 X-shape plates. In particular, the hysteretic behaviour of the DC has been modeled considering the Bouc&Wen model [48]-[49] with an elastic stiffness K_{el} and a ratio between the elastic and plastic stiffness $k = K_{el} / K_{pl}$. In Figure 7, the parameters of the Bouc&Wen model [48]-[49] are also reported for the DC with both LYP100 and S235 X-shape plates.

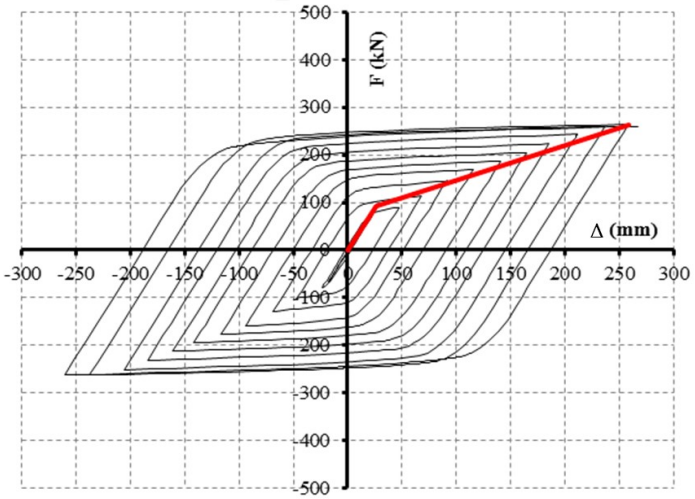

(a)

K_{el}	3560	N/mm
K_{pl}	738	N/mm
$k = K_{pl}/K_{el}$	0.207	
exp	10	

(b)

K_{el}	3630	N/mm
K_{pl}	609	N/mm
$k = K_{pl}/K_{el}$	0.168	
exp	10	

(c)

Figure 7: (a) Hysteretic behaviour of the DC using LYP100; Parameters of the Bouc&Wen [48]-[49] model for LYP100 (b) and S235 (c).

6 BUILDING MODEL EQUIPPED WITH THE DISSIPATIVE COLUMNS

As mentioned before, hysteretic dampers should be generally designed to yield before the primary structure, therefore their mechanical properties change along the building height. Assuming to have already established the shear strength of the primary system Q^i_{Fy}, mechanical properties of the i-th story may be summarized as follows [38],[50]:

$$Q^i{}_s = Q^i{}_{Fy} + Q^i{}_{Dy} \tag{17}$$

where Q^i_S, Q^i_{Fy}, and Q^i_{Dy} represent the yield shear strength of the entire system, primary structure and damping system respectively at the i-th story. Q^i_S and Q^i_{Fy} correspond to the relative displacement Δ^i_{Fy}, as well as Q^i_{Dy} corresponds to Δ^i_{Dy}. Defining Δ_{max} as the maximum story drift, μ_D and μ_F are, respectively, the story-drift ductility of the main frame and the story-drift ductility of the damper system. The lateral stiffness both of the primary structure and Dissipative Column system at the i-th story result being:

$$k^i{}_{Fy} = \frac{Q^i{}_{Fy}}{\Delta^i{}_{Fy}} \tag{18}$$

$$k^i{}_{Dy} = \frac{Q^i{}_{Dy}}{\Delta^i{}_{Dy}} \tag{19}$$

Defining the strength ratio β as the ratio of the yield strength of the damper system Q^i_{Dy} to that of the entire system Q^i_{Fy}, Q^i_{Dy} can be expressed as:

$$Q^i{}_{Dy} = \beta Q^i{}_s \tag{20}$$

$$Q^i{}_{Fy} = Q^i{}_s(1-\beta) \tag{21}$$

Moreover, the yield drift ratio ν can be defined as a ratio of damper yield drift to the one of the main structure, so, that the stiffness ratio κ is defined as:

$$\kappa = \frac{K^i{}_{Dy}}{K^i{}_{Fy}} = \frac{Q^i{}_{Dy}}{\Delta^i{}_{Dy}} \frac{\Delta^i{}_{Fy}}{Q^i_{Fy}} = \frac{\beta}{(1-\beta)\nu} \tag{22}$$

The damper strength ratio β and the yield story drift ratio ν are the main parameters useful to design the damping system. Passive control is achieved by yielding the dampers prior to the yield in the R/C frame, in other words, by setting the value of ν smaller than unity. The value of the drift ratio ν is defined from 0 to 1.0, and it is intended to be constant for all stories and strength ratios, according to "Constant yield story-drift ratio" scheme [38],[50]. The value ν=1.0 means that both the damper system and the main frame yield at the same story-drift level, and it can be assumed as the lowest protection to the main frame since the damper system will have the smallest stiffness and require larger story drifts to start to dissipate energy. To the scope to observe the influence of the DC on the seismic performance of an entire system, the nonlinear static and time history analyses, in SAP2000 [39], have been performed on the benchmark plane 10-story model [38],[50]. The benchmark plane model (Frame C) is represented in Figure 9 and the geometric and mechanical properties are described in [38],[50]. By means of the building regularity, the vertical distribution of lateral loads used for the eval-

uation of the pushover curve useful to design the DCs has been assumed proportional to the first mode shape [3].

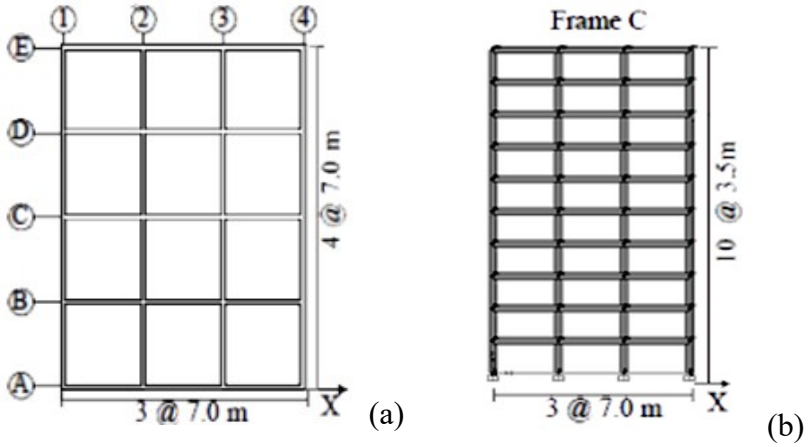

Figure 9: Typical plane (a) and elevation (b) benchmark model (modified from [38],[50]).

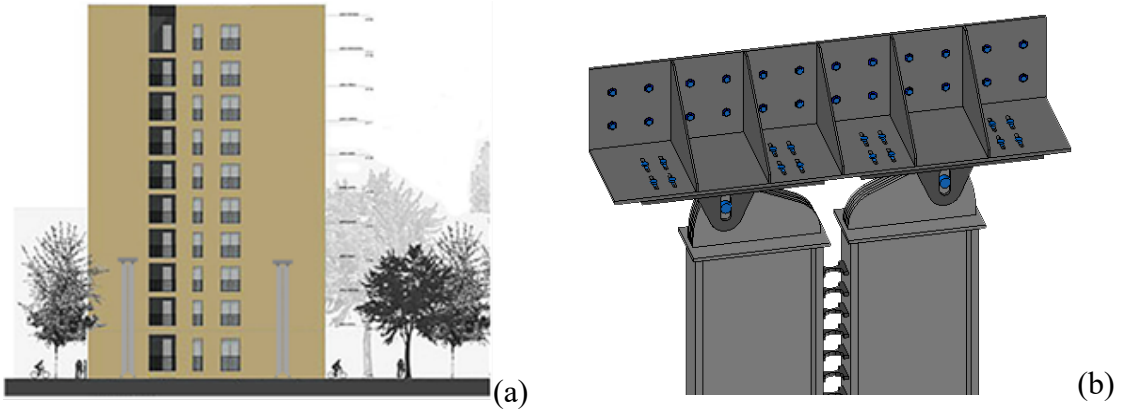

Figure 10: (a) Schematic installation of two DCs linked to the building; (b) Structural detail of the connection.

In the present study, two DCs have been applied between the third level and the ground. Figure 10 shows a schematic example of the connection between two DCs and the building and the structural detail of the link between the primary structure and damping system realized with two DCs so that both ones present the same deformation. Nonlinear analyses have been performed on the benchmark model with and without the DCs. The DCs have been modeled through nonlinear link element ruled by Bouc&Wen model, as described above, considering both LYP100 and S235 X-shape plates. The comparison between the bilinear pushover curve representative of the seismic response of the main frame in correspondence of the third level and the bilinear pushover curve descriptive of the seismic performance of the DCs with LYP100 and S235 X shape plates have allowed to determine the β and ν values for the considered system. As shown in Figure 11, the damper strength ratio β and the yield story drift ratio ν values are in accordance with the limit established by [38],[50] to obtain a good efficiency of the damper system. Considering the benchmark building located in L'Aquila site, within the "Direct Displacement Based Design" philosophy [3], the both DCs have been designed to increase the equivalent damping until to about 10% in addition to the inherent damping (5%) of the primary structure in order to achieve a target displacement between the roof and the ground equal about to 0.18 m. In particular, seven spectrum compatible input ground motions have been selected from the European database compatible in average with

the elastic spectrum (with viscous damping ξ = 5 %) relative to the ultimate limit state ULS, life safe, provided by the new Italian seismic code NTC08 [51] and considering an ordinary structure with a nominal life of 50 years located in L'Aquila (Italy), soil type C and topography class T2, to perform nonlinear time history analyses.

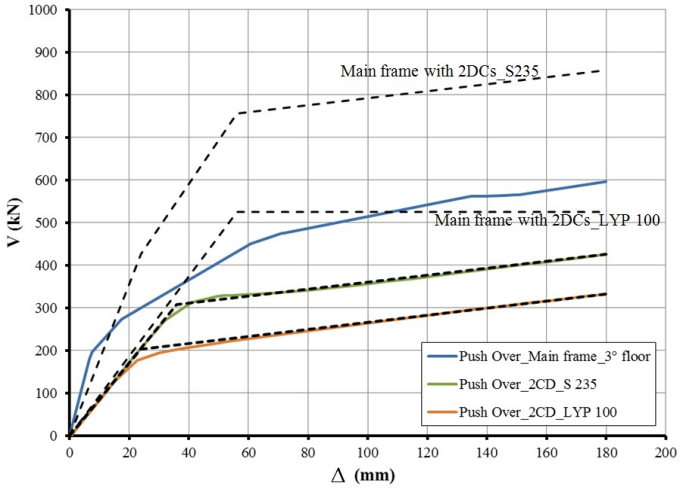

(a)

2 CD_LYP 100	2 CD_S 235
$\Delta'_{Dy} = 24\ mm$	$\Delta''_{Dy} = 36\ mm$

(b)

2 CD_LYP 100: ν = 0.28, β = 0.42

2 CD_S 235: ν = 0.38, β = 0.63

(c)

Figure 11: (a) Comparison between main frame pushover curve and DC pushover curves; Yielding displacements (b) and parameters [38],[50] (c) of the two DCs with LYP110 and S235 X-shape plates.

Waveform ID	Earthquake ID	Earthquake Name	M_w	Fault Mechnism	Epicentral Ditance [km]	PGA [m/s^2]
74	43	Gazli	6.7	thrust	11	6.0382
197	93	Montenegro	6.9	thrust	24	2.8797
290	146	Campano Lucano	6.9	normal	32	3.1662
535	250	Erzincan	6.6	strike slip	13	5.0275
1560	497	Duzce 1	7.2	oblique	39	7.3108
4673	1635	South Iceland	6.5	strike slip	15	4.6775
7329	2343	Faial	6.1	strike slip	11	4.1204

Table 3. Input ground motions.

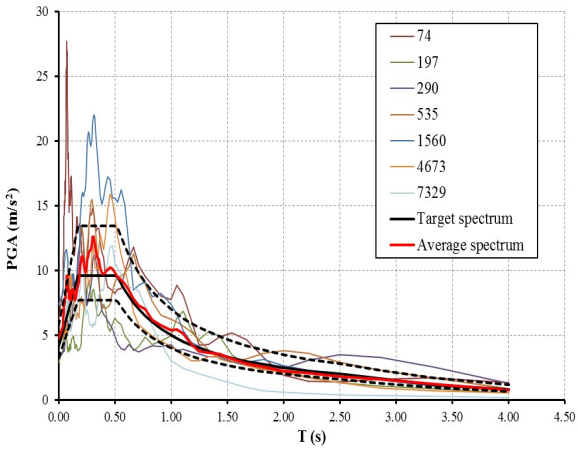

Figure 12: Response spectra of the selected ground motions and target spectrum (**ξ = 5 %**).

The values of the magnitude ranging from 6 to 8, and of the epicentral distance between 10 and 40 km are reported in Table 3. In Figure 12, the target spectrum as well as corresponding

elastic pseudo acceleration response spectra are shown. The time history analyses with and without the two DCs with LYP100 and S235 X shape plates linked to the main frame have been performed to evaluate the seismic performance in terms of relative displacements at each story. The effect of the damper system provided by the two DCs is significant until to 5-story and it is evident that the installation of two DCs to the 3rd story successfully affects the global seismic performance avoiding any soft stories and plastic hinges in the primary elements of the main frame.

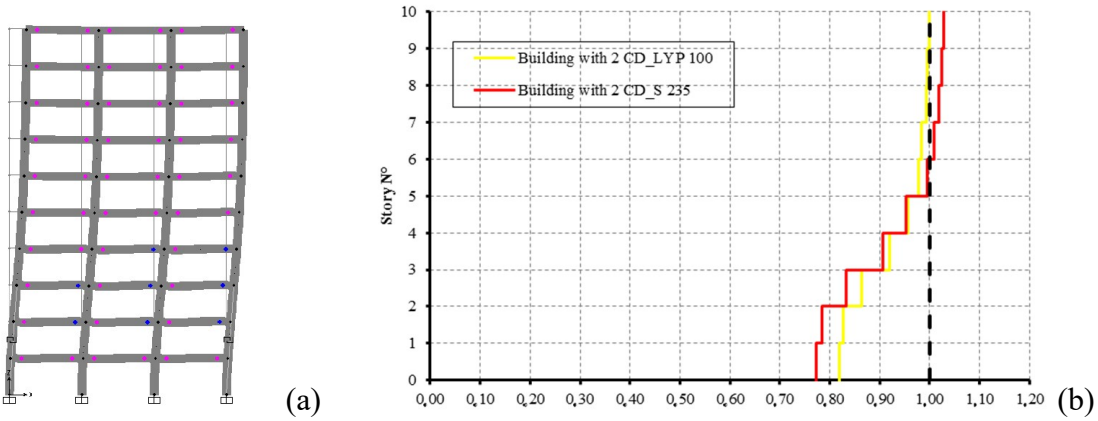

Figure 13: (a) Deformed Frame at the ultimate step (b) Normalized average maximum interstory drif ratio.

7 CONCLUDING REMARKS

The aim of this paper is to propose and investigate a new replaceable hysteretic damper consisting of two or more dissipative steel columns directly connected to two floors linked to each other with X-shaped low/mild steel plates. This element is able to add significant stiffness and damping to the structural system as well as to reduce seismic response and damage in primary structural members under severe earthquakes. The Dissipative Columns (DC) element equipped with both LYP100 and S235 X shape plates has been investigated through non-linear pushover and cyclic analyses. The efficiency of the proposed damper applied on a benchmark system has been investigated through time history analyses demonstrating successfully the benefits on the global seismic performance avoiding any soft stories and plastic hinges in the primary elements of the main frame.

REFERENCES

[1] M. De Iuliis, P. Castaldo, B. Palazzo, Analisi della domanda sismica inelastica del terremoto de L'Aquila su sistemi dimensionati secondo le NTC2008. *Ingegneria Sismica*, Patron Editore **XXVII**(3), 55–68, 2010.

[2] California Office of Emergency Services (OES). Vision 2000: Performance Based Seismic Engineering of Buildings; Structural Engineers Association of California: Sacramento, CA, USA, 1995.

[3] M.J.N. Priestley, Myths and fallacies in earthquake engineering-conflicts between design and reality. *Bull. NZNSEE*, **26**, 329–341,1993**.**

[4] P. Castaldo, B. Palazzo, P. Della Vecchia, Seismic reliability of base-isolated structures with friction pendulum bearings. *Engineering Structures,* **95**, 80-93, 2015.

[5] P. Castaldo, E. Tubaldi, Influence of FPS bearing properties on the seismic performance of base-isolated structures, *Earthquake Engineering and Structural Dynamics*, **44**(15), 2817–2836, 2015.

[6] B. Palazzo, P. Castaldo, P. Della Vecchia, Seismic reliability analysis of base-isolated structures with friction pendulum system, *2014 IEEE Workshop on Environmental, Energy and Struct. Monitoring Systems Proceedings*, Napoli, September 17-18, 2014.

[7] M.D. Symans, F.A. Charney, A.S. Whittaker, M.C. Constantinou, C.A. Kicher, M.W. Johnson, R.J. McNamara, Energy dissipation system for seismic applications: Current practise and recent developments. *J. Struct. Eng.*, **134**, 3–21, 2008.

[8] A. Wada, A. Watanabe, J. Connor, H. Kawai, M. Iwata, Damage Tolerant Structures. In *Proceeding of the Fifth US-Japan Workshop on the Improvement of Building Structural Design and Construction Procedures*, ATC-15, San Diego, CA, USA, 8–10 September 1992.

[9] R. Montuori, The influence of gravity loads on the seismic design of RBS connections, *Open Construction and Building Technology Journal*, **8**, 248-261, 2014.

[10] S. Pampanin, Emerging solutions for high seismic performance of precast-prestressed concrete buildings. *J. Adv. Concr. Technol.*, 3, 202–222, 2005.

[11] S. Pampanin, Reality-check and renewed challenges in earthquake engineering: Implementing low-damage structural systems-from theory to practice. In Proceeding of the *15WCEE*, Lisbon, Portugal, 24–28 September 2013.

[12] B. Palazzo, P. Castaldo, I. Marino, The steel column damper: a new hysteretic device providing additional stiffness and damping, *EUROSTEEL 2014*, September 10-12, Naples, Italy, 2014.

[13] B. Palazzo, P. Castaldo, I. Marino, The Dissipative Column: A New Hysteretic Damper," *Buildings* **5**(1), 163-178, 2015, doi:10.3390/buildings5010163.

[14] V. Piluso, R. Montuori, M. Troisi, Innovative structural details in MR-frames for free from damage structures, *Mechanics Research Communications*, **58**:146-156, 2014.

[15] P. Castaldo, M. De Iuliis, Optimal integrated seismic design of structural and viscoelastic bracing-damper systems, *Earthquake Engineering and Structural Dynamics*, **43**(12), 1809–1827, 2014, DOI: 10.1002/eqe.2425.

[16] P. Castaldo, *Integrated Seismic Design of Structure and Control Systems*. Springer International Publishing: New York, 2014 . DOI 10.1007/978-3-319-02615-2.

[17] A. Longo, R. Montuori, E. Nastri, V. Piluso, On the use of HSS in seismic-resistant structures, *Journal of Constructional Steel Research*, **103**:1-12, 2014.

[18] R. Montuori, R. Muscati, Plastic design of seismic resistant reinforced concrete frame," *Earthquake and Structures,* **8**(1), 205-224, 2015.

[19] Giugliano M.T., Longo A., Montuori R., Piluso V., Plastic design of CB-frames with reduced section solution for bracing members. *Journal of Constructional Steel Research.* Vol. 66 pp 611-621. 2010.

[20] Montuori R., Piluso V., Troisi M. Innovative structural details in MR-frames for free from damage structures *Mechanics Research Communications* – Vol. 58 pp. 146-156. 2014.

[21] Longo A., Montuori R., Piluso V., Theory of Plastic Mechanism Control of Dissipative Truss Moment Frames, *Engineering Structures*, Vol. 37, pp.

[22] Montuori, R. , Muscati, R. A General Procedure for Failure Mechanism Control of Reinforced Concrete Frames. Accepted for publication to Engineering Structures.

[23] Montuori, R., Nastri, E., Piluso, V., Theory of Plastic Mechanism Control for Eccentrically Braced Frames with inverted Y-scheme, *Journal of Constructional Steel Research*, Volume 92, pp. 122-135, 2014.

[24] Montuori, R., Nastri, E., Piluso, V., "Seismic Design of MRF-EBF Dual Systems with Vertical Links: Ec8 Vs Plastic Design", *Journal of Earthquake Engineering*, (2015)

[25] Montuori, R., Nastri, E., Piluso, V., "Seismic Response of EB-Frames with Inverted Yscheme: TPMC Versus Eurocode Provisions", *Earthquakes and Structures*, (2015)

[26] Longo A., Montuori R., Piluso V. Seismic Reliability of Chevron Braced Frames with Innovative Conception of Bracing Members, *Advanced Steel Construction, an International Journal* - Vol. 5, No. 4, December 2009.

[27] Longo, A. , Montuori, R., Piluso, V Theory of plastic mechanism control for MRF–CBF dual systems and its validation

[28] Bulletin of Earthquake Engineering. Volume 12, Issue 6, 6 November 2014, Pages 2745-2775

[29] R. Montuori, E. Nastri, V. Piluso, Theory of plastic mechanism control for the seismic design of braced frames equipped with friction dampers, *Mechanics Research Communications* **58**:112-123, 2014.

[30] R. Montuori, E. Nastri, V. Piluso, Advances in theory of plastic mechanism control: Closed form solution for MR-Frames, *Earthquake Engineering and Structural Dynamics,* **44**(7):1035-1054, 2015.

[31] M. De Iuliis, P. Castaldo, An energy-based approach to the seismic control of one-way asymmetrical structural systems using semi-active devices, *Ingegneria Sismica - International Journal of Earthquake Engineering* **XXIX**(4):31-42, 2012.

[32] J. Kim, Y. Seo, Seismic design of low-rise steel frames with buckling-restrained Braces. *Eng. Struct.*, **26**, 543–551, 2004.

[33] K.A.S. Susantha, T. Aoki, T. Kumano, K. Yamamoto, Application of Low-Yield Strength Steel in Steel Bridge Piers, In Proceeding of the *13th WCEE*, Vancouver, BC, Canada, 1–6 August 2004.

[34] Montuori R. The Influence of Gravity Loads on the Seismic Design of RBS Connections. *The Open Construction and Building Technology Journal*, 2014, 8, (Suppl 1: M6) 248-261.

[35] Montuori, R. Design of "Dog-bone" connection: The role of vertical loads. COMPDYN 2015 - 5th ECCOMAS Thematic Conference on Computational Methods in Structural Dynamics and Earthquake Engineering 2015, Pages 3368-3387. Crete; Greece; 25 May 2015 through 27 May 2015.

[36] ABAQUS, User's Manual: Volume III: Materials, 2010.

[37] ABAQUS, User's Manual: Volume IV: Elements, 2010.

[38] A.J.A. Oviedo, M. Midorikawa, T. Asari, Earthquake response of ten-story story-drift-controlled reinforced concrete frames with hysteretic dampers. *Eng. Struct.*, **32**, 1735–1746, 2010.

[39] SAP2000 vers; Computers Structures Inc.: Berkeley, CA, USA, 2010.

[40] A. Ghobarah, On Drift Limits Associated with Different Damage Levels. In Proceedings of the International *Workshop on Performance-Based Seismic Design, Department of Civil Engineering*, McMaster University, Bled, Slovenia, 28 June–1 July 2004.

[41] I. Aiken, D. Nims, A. Whittaker, J. Kelly, Testing of passive energy dissipation systems. *Earthq. Spectra Earthq. Eng. Res. Inst. Calif.*, **9**, 335–370, 1993.

[42] A. Whittaker, V. Bertero, J. Alonso, Thompson, C. *Earthquake Simulator Testing of Steel Plate Added Damping and Stiffness Elements*. Report No. UCB/EERC-89/02; Earthquake Eng. Research Center, University of California, Berkeley, CA, USA, 1989.

[43] A.S. Whittaker, V.V. Bertero, Thompson, C.L., Alonso, L.J. Seismic testing of steel plate energy dissipation devices. *Earthq. Spectra*, **7**, 563–604, 1991.

[44] CEN-European Committee for Standardization *Eurocode 3 Part 1: General Rules and Rules for Buildings*, Brussels, Belgium., 2007.

[45] E. Saeki, M. Sugisawa, T. Yamaguchi, A. Wada, Mechanical properties of low yield point steels," *J. Mater. Civ. Eng.* **10**, 143-152, 1998.

[46] A. Tena-Colunga, Mathematical modelling of the ADAS energy dissipation device, *Engineering Structures* **19**(10), 811-821, 1997.

[47] V. Piluso, C. Faella, G. Rizzano Ultimate behavior of bolted T-stubs. Part I: theoretical model. *J Struct Eng* ASCE, **127**(6), 686–93, 2001.

[48] R. Bouc, Forced vibration of mechanical systems with hysteresis. Proceedings of the 4th Conference on Nonlinear Oscillations, Prague, Czechoslovakia, 315-315, 1967.

[49] YK. Wen, Method for random vibration of hysteretic systems. *Journal of the Engineering Mechanics Division*, **102**(2), 249-263, 1976.

[50] A.J.A. Oviedo, M. Midorikawa, T. Asari, Performance of Story-Drift-Controlled R/C Frames Equipped with Hysteretic Dampers Subjected to Earthquake Motions. 15 WCEE, Lisboa 2012.

[51] NTC08 - Norme tecniche per le costruzioni, Gazzetta Ufficiale del 04.02.08, DM 14.01.08, Ministero delle Infrastrutture, 2008.